Insights Into the Dynamics of Coupled VO 2 Oscillators for ONNs

Juan Núñez, José M. Quintana, María José Avedillo de Juan, Manuel Jiménez Través, Aida Todri-Sanial, Elisabetta Corti, Siegfried Karg, Bernabé Linares-Barranco

HAL Id: lirmm-03432278

https://hal-lirmm.ccsd.cnrs.fr/lirmm-03432278

Submitted on 17 Nov 2021

Insights Into the Dynamics of Coupled VO$_2$ Oscillators for ONNs

Juan Núñez[ID], José M. Quintana, María J. Avedillo[ID], Manuel Jiménez[ID], Aida Todri-Sanial[ID], Elisabetta Corti[ID], Siegfried Karg[ID], *Senior Member, IEEE*, and Bernabé Linares-Barranco

Abstract—The collective behavior of many coupled oscillator systems is currently being explored for the implementation of different non-conventional computing paradigms. In particular, VO$_2$ based nano-oscillators have been proposed to implement oscillatory neural networks that can serve as associative memories, useful in pattern recognition applications. Although the dynamics of a pair of coupled oscillators have already been extensively analyzed, in this brief, the topic is addressed more practically. Firstly, for the application mentioned above, each oscillator needs to be initialized in a given phase to represent the input pattern. We demonstrate the impact of this initialization mechanism on the final phase relationship of the oscillators. Secondly, such oscillatory networks are based on frequency synchronization, in which the impact of variability is critical. We carried out a comprehensive mathematical analysis of a pair of coupled oscillators taking into account both issues, which is a first step towards the design of the oscillatory neural networks for associative memory applications.

Index Terms—Phase transition materials, VO$_2$, Nano-oscillators, ONNs, coupled oscillators, phase locking.

I. INTRODUCTION

THE COLLECTIVE behavior of many coupled oscillator systems is currently being explored for the implementation of different non-conventional computing paradigms [1]–[12]. Interest in this approach has been fueled by the emergence of a number of very different devices that enable the implementation of compact and energy-efficient oscillators. Examples include microelectromechanical systems (MEMS), spin-torque oscillators (STO), or phase transition materials (PTMs). In [11], many oscillators are evaluated as potential building blocks for oscillatory computing architectures. In terms of energy, relaxation
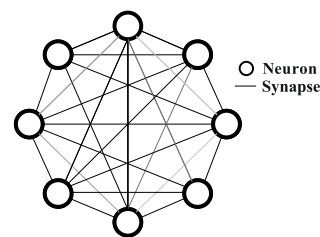
Fig. 1. Hopfield Neural Network (HNN). Based on this scheme, OHNNs are designed by replacing the neurons by oscillators and the synapses by coupling resistors.

oscillators based on PTMs exhibit good performance. They rank second (together with spin-hall oscillators), just behind superconducting oscillators. The compound most widely used as PTM is vanadium dioxide (VO$_2$). So different groups are exploring the capability of a VO$_2$ device in series with a resistor to oscillate in the implementation of electrically-coupled-oscillator-based processing [1]–[8]. Both resistive and capacitive coupling has been explored.

Among other applications, coupled oscillator systems have been applied as associative memories for pattern recognition using a Hopfield-type architecture (or Hopfield Neural Network, [13]) [14]–[16]. This brief looks at using VO$_2$ oscillator networks working with weak resistive coupling. In [5], the neurons in a fully connected HNN (Fig. 1) were replaced by VO$_2$ oscillators, with weak resistive coupling between them representing synapse weights. These Oscillatory Hopfield Neural Networks (OHNN) were proposed to perform tasks such as image recognition through the suitable tuning of resistance values.

An in-depth understanding of the dynamics of coupled VO$_2$ oscillators is critical when addressing OHNNs. The issue has been studied in the literature [17], [18]. In [17], two identical coupled oscillators were analyzed and the phase relationship to which they converge, in-phase or antiphase, was derived as a function of the coupling resistance and capacitance. The discussion focused more on the relative strength of resistive and capacitive coupling, leading to in-phase when resistive coupling dominates and to anti-phase when capacitive coupling dominates. However, no insights were offered into weak resistive coupling. In [4], it was shown both experimentally and by simulation that both in-phase and anti-phase can be obtained for a pair of resistively coupled VO$_2$ oscillators. In this brief, we further extend this work numerically and perform an in-depth analysis by means of design space exploration experiments. This analysis was motivated by the idea of the aforementioned associative memory application. In that context, each oscillator must be initialized in a given phase to
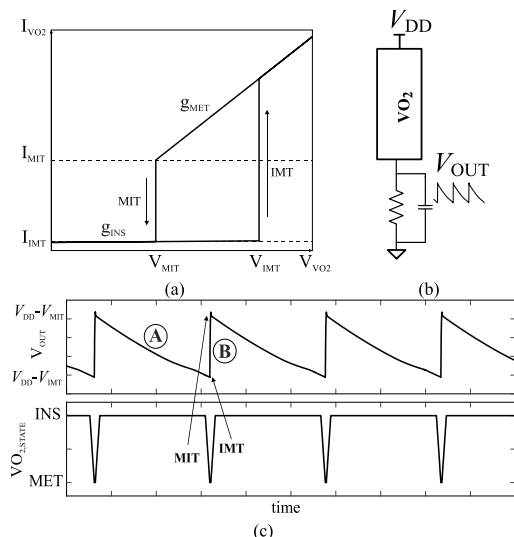
Fig. 2. (a) Generic I-V curve of a VO$_2$ device. VO$_2$ oscillator (b) circuit topology, (c) operation waveforms in which points corresponding to insulator-to-metal and metal-to-insulator transitions have been marked with arrows.

represent the input pattern, so we also demonstrate the impact of this initialization mechanism on the final phase relationship of the oscillators. In this regard, we show that the initialization process provides agile, efficient knowledge of how coupled oscillators operate. Also, such oscillatory networks are based on frequency synchronization, for which the impact of variability is a critical factor. Taking into account that the two oscillators are not actually identical, we were able to quantify previous findings related to the coupling strength required to achieve synchronization. Finally, we discuss how the analysis carried out is useful for deriving design guidelines for OHNNs.

This brief is organized as follows. Section II describes the operation of VO$_2$ oscillators and Oscillatory HNNs. Section III deals with the analysis methodology for the two coupled oscillators we used. In Section IV we apply our analysis tool for design space exploration. Finally, some conclusions are drawn in Section V.

II. BACKGROUND

A. VO$_2$ Based Oscillator

VO$_2$ undergoes insulator-metal transitions under given electrical stimuli. That is, abrupt switching is experienced from/to a high resistivity state (insulating phase) to/from a low resistivity state (metallic phase). Under no electrical stimuli, VO$_2$ tends to stabilize in the insulating phase. When the applied voltage increases and the current density flowing through it reaches $J_{C\text{-}IMT}$, insulator-to-metal transition (IMT) occurs. Once in the metallic state, when the voltage decreases and the current density drops below $J_{C\text{-}MIT}$, metal-to-insulator transition (MIT) takes place. Fig. 2a shows the I-V characteristic of a generic VO$_2$ device. In this work, we use the VO$_2$ device with the electrical parameters shown in Table I [5]. V_{IMT} (V_{MIT}) is the voltage at which the insulator-to-metal transition, (IMT) (metal-to-insulator transition, MIT) occurs. R_{INS} (R_{MET}) is the resistance in the insulating (metallic) state. Since MIT and IMT transitions are abrupt but not instantaneous, transition times (TT$_{IMT}$, TT$_{MIT}$) are also considered.

Fig. 2b shows a VO$_2$ based oscillator [17], [19]. Fig. 2c depicts waveforms for the oscillator output. The state of the

TABLE I
VO$_2$ ELECTRICAL PARAMETERS

V_{IMT}	V_{MIT}	R_{MET}	R_{INS}	TT$_{IMT}$/TT$_{MIT}$
1.99V	0.99V	0.99KΩ	100.2KΩ	30ns

VO$_2$ is also shown to better illustrate the circuit behavior. VO$_{2,STATE}$ = 'INS' means the device is in the insulating state. VO$_{2,STATE}$ = 'MET' corresponds to the device in the metallic state. Assuming the VO$_2$ is in an insulating state (marked with "A" in Fig. 2c), the oscillator output is discharged through the resistor. This increases the voltage drop across the VO$_2$ ($V_{DD} - V_{OUT}$) and so current through it increases. Once enough current density circulates ($J_{C\text{-}IMT}$), it switches to the metallic state (marked with "B" in Fig. 2c). Equivalently, using the electrical model, switching to the metallic state occurs once the VO$_2$ voltage reaches V_{IMT}. The capacitor is then charged through the VO$_2$. This charging is very fast because of the low R_{MET} value. The voltage seen by the VO$_2$ decreases until it reaches V_{MIT} and the metal-to-insulator state transition occurs.

B. OHNNs and Smart Initialization Mechanism

The Oscillatory HNN proposed in [4]–[7] replaces the neurons in the HNN (Fig. 1) with VO$_2$ oscillators, with weak resistive coupling between them representing synapse weights. It has been demonstrated [5], [7] that such OHNN is suitable for performing tasks as image recognition. This network works as an associative memory applicable for pattern recognition. The state of the network is defined by the phase of each neuron. Some states are stable while others, if entered, converge to a stable one. For pattern recognition, a set of patterns (called training patterns) are stored in the network. For that, the network is configured in such a way that the states corresponding to those patterns are stable. When the network is placed in a state corresponding to a distorted version of a training pattern, it evolves to a training one, ideally to the most similar one. The initial state of the network thus acts as the applied input pattern. Configuration involves setting suitable values for the interconnection resistances. Resistances play the role of the weights in the conventional HNN. Different rules can be used to derive the set of required weights for storing a given set of patterns. However, in the OHNN, it is not enough with this rule, but the weights must be additionally mapped to resistance values. For this, a thorough understanding of how oscillators interact and how coupling affects their behavior is essential.

The authors proposed forcing a given initial state by selectively delaying the supply voltage of each neuron [5], [6]. For example, assuming only binary patterns are applied, such as black and white pixel images, the initial state of the network has only two different phases, 180° apart. Those oscillators corresponding to black pixels are in one phase and those corresponding to white ones are in the other phase. To achieve this, the black oscillators are switched on at T_0 and the white ones at $T_0 + T_{OSC}/2$, where T_{OSC} is the period of the oscillations. A larger number of different phases (and therefore switching delays) are used if grey-coded images are to be processed (non-binary input patterns). Fig. 3 shows the initialization of two resistively coupled oscillators in which applying different delays between the supply voltages of each neuron produces different behaviors. In Fig. 3a the delay is 0.1·T_{OSC}, leading to in-phase operation, whereas in Fig. 3b anti-phase operation
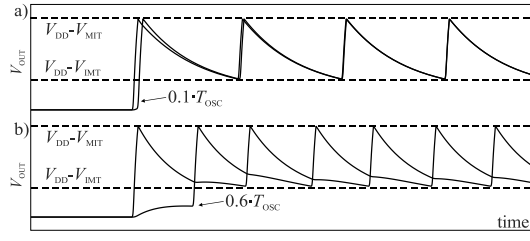
Fig. 3. Final state of two coupled oscillators for two values of the delay between the switching of their supply voltages. (a) In-phase fpr delay equal to $0.1 \cdot T_{OSC}$. (b) Anti-phase for delay equal to $0.6 \cdot T_{OSC}$. The two plots have been obtained using the same value of R_C and $C_C = 0.05pF$. Same results are obtained by eliminating C_C.

Fig. 4. Equivalent circuit of two coupled VO_2 oscillators with an $R_C C_C$ circuit used as the coupling circuit.

is achieved for a delay of $0.6 \cdot T_{OSC}$. Note that a single coupling resistance value enables both in-phase and anti-phase final states depending on the initialization process. This is a bistable behavior that is attractive for pattern recognition.

Note that previously reported OHNNs which also use resistances for synapses [20], [21] implement a negative weight between a neuron i and a neuron j as a positive one between the output of the neuron i (neuron j) shifted by 180° (the oscillator output is inverted) and the neuron j (neuron i). The resistance value encodes the weight absolute value but not the sign. In contrast to this, the proposed network is based on the rich and complex dynamics of weakly coupled oscillators; hence, this work focuses on a thorough exploration of the design spaces of two coupled oscillators, taking into account the initialization mechanism and the impact of variability. Later, the study of the training process will be done on the basis of the insights from this work.

III. MATHEMATICAL ANALYSIS

The mathematical analysis of the dynamics of coupled VO_2 oscillators uses the equivalent circuit in Fig. 4. Note that, for generality, a coupling with both resistance and capacitance is assumed. The conductances involved are $g_{MET} = R_{MET}^{-1}$, $g_{INS} = R_{INS}^{-1}$, $g_S = R_S^{-1}$, and $g_C = R_C^{-1}$ (see Section II-A). The equation for the single oscillator dynamics can be written as:

$$CV' = \begin{cases} (V_{DD}\text{-}V_{OUT})g_{MET}\text{-}Vg_S & \text{charging [C]} \\ (V_{DD}\text{-}V_{OUT})g_{INS}\text{-}Vg_S & \text{discharging [D]} \end{cases} \quad (1)$$

Effective charging occurs through g_{MET} but there is added leakage through g_S, whereas effective discharging occurs through g_S and there is also current injection from g_{INS}.

When two oscillators are coupled in the manner described in Fig. 4, the system can be described using eq. (1) for each of them, but considering the coupling current ($I_{C1} = -I_{C2}$), which is given by:

$$I_{C1} = (V'_{OUT,1}\text{-}V'_{OUT,2})C_C + (V_{OUT,1}\text{-}V_{OUT,2})g_C \quad (2)$$

leading to

$$C_1 V'_{OUT,1} = \begin{cases} (V_{DD}(t)\text{-}V_{OUT,1})g_{MET1}\text{-}V_{OUT,1}g_{S1}\text{-}I_{C1} & \text{[C]} \\ (V_{DD}(t)\text{-}V_{OUT,1})g_{INS1}\text{-}V_{OUT,1}g_{S1}\text{-}I_{C1} & \text{[D]} \end{cases} \quad (3)$$

$$C_2 V'_{OUT,2} = \begin{cases} (V_{DD}(t)\text{-}V_{OUT,2})g_{MET2}\text{-}V_{OUT,2}g_{S2}\text{-}I_{C2} & \text{[C]} \\ (V_{DD}(t)\text{-}V_{OUT,2})g_{INS2}\text{-}V_{OUT,2}g_{S2}\text{-}I_{C2} & \text{[D]} \end{cases} \quad (4)$$

where different capacitance C, g_{MET}, g_{INS}, and g_S are used for each oscillator, making it possible to explore intra-chip variability. Also note that V_{DD} is a function of time, allowing
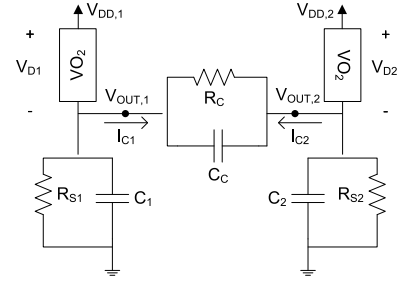
the initialization mechanism described in the previous section to be modeled.

Expressing the charging and discharging conditions in terms of $I - V$ driving point characteristics for the VO_2 device, the following relationships can now be derived to determine whether the device is in the metallic state (during charging) or in the insulating state (during discharging):

$$\begin{cases} (V_{MIT} \leq |V_{DD}\text{-}V_{OUT,i}| \leq V_{IMT}) \wedge (V'_{OUT,i} \geq 0) \vee |V_{DD}\text{-}V_{OUT,i}| \geq V_{IMT} & \text{[C]} \\ (V_{MIT} \leq |V_{DD}\text{-}V_{OUT,i}| \leq V_{IMT}) \wedge (V'_{OUT,i} \leq 0) \vee |V_{DD}\text{-}V_{OUT,i}| \leq V_{MIT} & \text{[D]} \end{cases}$$

$$(5)$$

where $\wedge$ and $\vee$ are the symbols for logical AND and OR, and $i \in \{1, 2\}$. Note the use of the derivative to model hysteresis. When the applied voltage is between the threshold voltages (V_{MIT} and V_{IMT}), there is hysteresis (see Fig. 2a) and so it needs to be distinguished whether the voltage is increasing or decreasing. This is not required when the applied voltage is outside the hysteresis region (right-hand side of $\vee$ operator).

This mathematical analysis served as a starting point to develop a toolbox in the MATLAB environment that allows the systematic exploration of design spaces in two coupled oscillators using VO_2 devices. Equations (3) and (4) are solved while concurrently determining the states of the VO_2 devices through Equation (5). As far as we know, this is the first time that a study has addressed the incorporation of variability and the initialization mechanisms using supply voltage delay.

By simulating the operation of the two coupled oscillators and processing the results, we were able to evaluate interesting features of the two-oscillator systems, including synchronization detection, measurement of operating frequency, phase differences when synchronization is achieved, and settling time.

It is worth mentioning that the tool incorporates a first step in which it is identified whether the two oscillators couple in-phase or not. This is done simply by analyzing the very first cycles, as described below, and leads to time savings when exploring design spaces.

In-phase or anti-phase operation is closely linked to the oscillators' initialization process, and more specifically to what happens the first time that both oscillator outputs fall down to $V_{DD}\text{-}V_{IMT}$ (both VO_2 devices operating in an insulating state). Fig. 5 illustrates this idea by showing an example in which both oscillators are initialized with a quarter-period difference and two R_C values: one forcing an in-phase operation (7KΩ in Fig. 5a) and the other anti-phase (30KΩ in Fig. 5b). The scenario in Fig. 5a shows that the strong coupling between the two oscillators forces that after the first time the oscillator outputs fall down, the difference between the switching
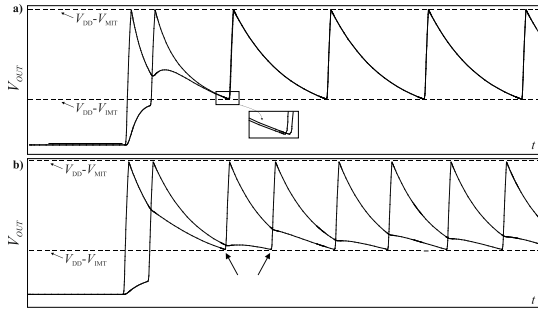
Fig. 5. Initialization of two coupled oscillators for two values of the coupling resistance (Cc = 0.05pF). (a) Convergence to in-phase operation: both VO$_2$ oscillators switch to metallic state closer than during initialization (b) Convergence to anti-phase operation: state transitions are spaced out in time. Same results are obtained by eliminating C$_C$.
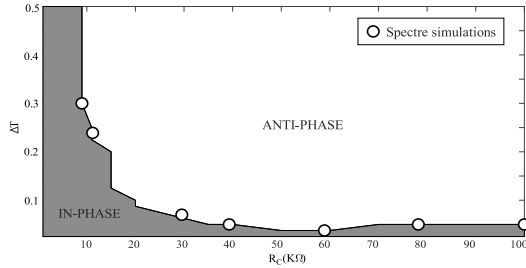

Fig. 6. ΔT vs. R$_C$ plot in which in-phase and anti-phase operation regions are identified. Spectre simulations are marked with circles, showing close correspondence between the results obtained by electrical simulations and by the tool.

times to metallic state of the VO$_2$ devices of both oscillators is less than the initial delay, and that this behavior is maintained thereafter. In the situation shown in Fig. 5b, the times when the switching between states occurs in each oscillator tend to move further apart. Thus, the transitions to the metallic state, marked with arrows in the figure, occur with a time difference greater than that corresponding to initialization: note that once that the VO$_2$ device of the first oscillator switches to the metallic state, its output voltage is higher than the voltage at the output of the other oscillator and, therefore, there is a current flow through the coupling network from the former to the latter which slows down the discharge of its capacitor and delays its VO$_2$ switching to metallic.

Based on this observation, the tool is able to determine in the first cycles of oscillation whether the oscillators will end up being in-phase.

IV. DESIGN SPACE EXPLORATION. CASE STUDY

The analysis tool was applied to explore the dynamics of two coupled oscillators. These simulations used the VO$_2$ device reported in Table I and oscillator resistance and capacitance values of 13KΩ and 100pF, respectively. The supply voltage of both oscillators was set to 2.5V.

First, a design space was analyzed where the variables were the time difference between oscillator initialization (ΔT) and coupling resistance (R$_C$). Nominal values were used for all design parameters. R$_C$ was explored because our target OHNN used resistive coupling. However, a very small coupling capacitance set to 0.05pF was included to model parasitic in the actual circuit.

Fig. 6 shows the plot generated by the toolbox indicating whether the oscillators were in-phase or anti-phase (180°).
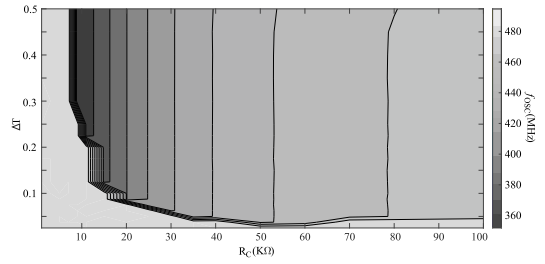

Fig. 7. ΔT vs. R$_C$ plot for oscillation frequency. Note that the same oscillation frequency is observed for the in-phase region. In the anti-phase region, stronger coupling (smaller R$_C$ values) leads to smaller oscillation frequency values.

The values explored for ΔT ranged from zero to half the period of the isolated oscillator, while for R$_C$ a range of values (1KΩ-100KΩ) was covered, including strong and weak coupling conditions. The in-phase operation region covered a wide range of ΔT values for lower R$_C$ values (strong coupling between the oscillators). However, when the coupling was very weak, the in-phase operation was only possible when both oscillators were initialized almost simultaneously. Fig. 6 also includes a curve obtained from the points marking the limit between the in-phase and anti-phase regions, obtained by electrical simulations using the Spectre simulator and by an in-house Verilog-A model for the VO$_2$ validated against experimental data [5]. Note the close correspondence between the results provided by the tool and those obtained by electrical simulations.

Also, a region in which the final phase relationship depends on initial delay can be identified. On its basis, this simplest 2-neuron OHNN can be configured to have two stable states: one with the two neurons in phase and the other with them anti-phase, i.e., we can store a pattern with two equal pixels and another one with one black and one white pixel. Gray input patterns evolve to one of them depending on how different the gray levels of the two pixels are. This is exactly what is shown in Fig. 3. The oscillators end up in-phase (top) or anti-phase (bottom) depending on the initialization delay and initialization delays encode gray levels. If the first oscillator to switch on is taken as white, input pattern in a) correspond to white pixel and light gray one while b) corresponds to white and dark gray. For that, an R$_C$ value into this bistability region is selected (R$_C$ close to 10KΩ – 15KΩ).

The results for operating frequency are shown in Fig. 7. As expected, oscillators operating in phase do so at a frequency equal to that of the isolated oscillator (about 490MHz). However, it is interesting to study the behavior of the oscillating frequency for the anti-phase region, especially the abrupt transition that occurs between the in-phase and anti-phase operating frequencies. For the anti-phase final state, stronger coupling (smaller R$_C$ values) leads to smaller oscillation frequency.

Finally, Fig. 8 provides the results corresponding to the settling time. The in-phase behavior stabilizes in the first cycles of oscillation, so the shortest times are therefore associated with it. In contrast, for anti-phase operation, the stronger the coupling between the oscillators and the closer ΔT is to half the period, the less time it will take for the steady-state to be established. For that reason, the longer settling times are in the lower right corner.

As reported by [4], [5], variability in the fabrication of VO$_2$ devices can affect operation at circuit level. Here we will
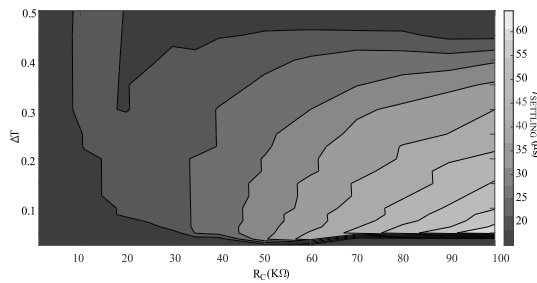
Fig. 8. ΔT vs. R_C plot for settling time. In-phase synchronization is faster than out of phase synchronization. Settling time increases for smaller coupling strength and smaller initialization delay.
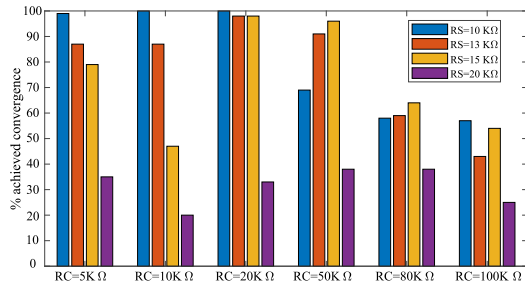

Fig. 9. Bar chart representing the percentage of cases where the oscillators have been successfully synchronized in frequency for different values of coupling resistance (R_C) and oscillator resistance (R_S).

exploit the toolbox described above to analyze how the variability of the VO_2 device's electrical parameters impacts the operation of the two coupled oscillators. In particular, we will force variations in the insulating and metallic resistances of the VO_2 devices. A Monte Carlo experiment has been carried out in which the VO_2 resistances take values assuming a normal Gaussian distribution ($\sigma = \pm 10\%$ around the nominal values). This makes the frequency of the two oscillators unequal, which may prevent synchronization. Unlike the results shown in Fig. 7, synchronization is not achieved in all cases. Fig. 9 shows the fraction of cases in which synchronization is achieved for different oscillator resistance and coupling resistance values. Coupled oscillators with different R_S values (10KΩ, 13KΩ, 15KΩ and 20KΩ) and the same C value (100pF), i.e., with different nominal operating frequencies, have been explored. The results show that, for stronger couplings scenarios ($R_C \leq 20K\Omega$), as R_S decreases, convergence is improved, and almost all experiments synchronize for $R_S = 10K\Omega$. In the region of weaker couplings ($R_C \geq 80K\Omega$) there is a significant drop in the number of cases that converge. For $R_S = 20K\Omega$ the results are significantly worse than the others in the explored range of R_C.

These results quantify the impact of the variability of two of the VO_2 device's electrical parameters into the synchronization phenomena and suggest that the oscillator design should also take into account variability to be able to tolerate it without preventing synchronization. Our results show that the oscillator design is critical for the 2-neuron system performance.

V. CONCLUSION

The dynamics of two electrically resistively coupled VO_2 oscillators were analyzed in-depth. Our results are in agreement with previous experimental results showing that enough weak resistive coupling pushes both oscillators out of phase and slightly modifies oscillation frequency and settling time. Additionally, our analysis gives an insight into the relationship

between key design parameters for achieving synchronization under variability. We have illustrated that in OHNNs resistance values are responsible for enabling the suitable coupling dynamic to achieve associative memory operation. The information obtained from this study shall inspire us to explore a rule to map the weights of the HNN to the resistance values of the OHNN. A rule which maps positive weights to the right part of the bistability region and negative ones to the left, together with a scaling of the resistance values according to the network size, shall be explored for the design of OHNNs.

REFERENCES

[1] N. Shukla et al., "Pairwise coupled hybrid vanadium dioxide-MOSFET (HVFET) oscillators for non-Boolean associative computing," in Proc. IEEE Int. Electron Devices Meeting, San Francisco, CA, USA, 2014, pp. 1–4.

[2] M. J. Avedillo, J. M. Quintana, and J. Núñez, "Phase transition device for phase storing," IEEE Trans. Nanotechnol., vol. 19, pp. 107–112, Jan. 2020. [Online]. Available: https://ieeexplore.ieee.org/document/8960534

[3] W. Yi, K. K. Tsang, S. K. Lam, X. Bai, J. A. Crowell, and E. A. Flores, "Biological plausibility and stochasticity in scalable VO_2 active memristor neurons," Nat. Commun., vol. 9, pp. 1–10, Nov. 2018.

[4] E. Corti, B. Gotsmann, K. Moselund, A. M. Ionescu, J. Robertson, and S. Karg, "Scaled resistively-coupled VO_2 oscillators for neuromorphic computing," Solid-State Electron., vol. 168, Jun. 2020, Art. no. 17729.

[5] E. E. Corti, B. Gotsmann, K. Moselund, I. Stolichnov, A. Ionescu, and S. Karg, "Resistive coupled VO2 oscillators for image recognition," in Proc. IEEE Int. Conf. Rebooting Comput. (ICRC), McLean, VA, USA, 2018, pp. 1–7.

[6] E. Corti et al., "Time-delay encoded image recognition in a network of resistively coupled VO2 on Si oscillators," IEEE Electron Device Lett., vol. 41, no. 4, pp. 629–632, Apr. 2020.

[7] E. Corti et al., "VO_2 oscillators coupling for neuromorphic computation," in Proc. Joint Int. EUROSOI Workshop Int. Conf. Ultimate Integr. Silicon (EUROSOI-ULIS), Grenoble, France, 2019, pp. 1–4.

[8] A. Parihar, N. Shukla, M. Jerry, S. Datta, and A. Raychowdhury, "Vertex coloring of graphs via phase dynamics of coupled oscillatory networks," Sci. Rep., vol. 7, p. 911, Apr. 2017.

[9] A. Ascoli, S. Slesazeck, H. Mähne, R. Tetzlaff, and T. Mikolajick, "Nonlinear dynamics of a locally-active memristor," IEEE Trans. Circuits Syst. I, Reg. Papers, vol. 62, no. 4, pp. 1165–1175, Apr. 2015.

[10] G. A. Gibson et al., "An accurate locally active memristor model for S-type negative differential resistance in NbO$_x$," Appl. Phys. Lett., vol. 108, no. 2, 2016, Art. no. 023505.

[11] G. Csaba and W. Porod, "Coupled oscillators for computing: A review and perspective," Appl. Phys. Rev., vol. 7, Jan. 2020, Art. no. 011302.

[12] A. Raychowdhury et al., "Computing with networks of oscillatory dynamical systems," Proc. IEEE, vol. 107, no. 1, pp. 73–89, Jan. 2019.

[13] J. J. Hopfield, "Neural networks and physical systems with emergent collective computational abilities," Proc. Nat. Acad. Sci. USA, vol. 79, no. 8, pp. 2554–2558, 1982.

[14] F. C. Hoppensteadt and E. M. Izhikevich, "Oscillatory neurocomputers with dynamic connectivity," Phys. Rev. Lett., vol. 82, no. 14, pp. 2983–2986, Apr. 1999.

[15] D. E. Nikonov et al., "Coupled-oscillator associative memory array operation for pattern recognition," IEEE J. Explor. Solid-State Computat. Devices Circuits, vol. 1, pp. 85–93, Dec. 2015. [Online]. Available: https://ieeexplore.ieee.org/document/7337390

[16] R. Follmann, E. E. N. Macau, E. Rosa, and J. R. C. Piqueira, "Phase oscillatory network and visual pattern recognition," IEEE Trans. Neural Netw. Learn. Syst., vol. 26, no. 7, pp. 1539–1544, Jul. 2015.

[17] A. Parihar, N. Shukla, S. Datta, and A. Raychowdhury, "Synchronization of pairwise-coupled, identical, relaxation oscillators based on metal-insulator phase transition devices: A model study," J. Appl. Phys., vol. 117, no. 5, 2015, Art. no. 054902.

[18] V. V. Perminov, V. V. Putrolaynen, M. A. Belyaev, and A. A. Velichko, "Synchronization in the system of coupled oscillators based on VO2 switches," J. Phys. Conf., vol. 929, no. 1, 2017, Art. no. 12045.

[19] P. Maffezzoni, L. Daniel, N. Shukla, S. Datta, and A. Raychowdhury, "Modeling and simulation of vanadium dioxide relaxation oscillators," IEEE Trans. Circuits Syst. I, Reg. Papers, vol. 62, no. 9, pp. 2207–2215, Sep. 2015.

[20] T. Jackson, S. Pagliarini, and L. Pileggi, "An oscillatory neural network with programmable resistive synapses in 28 nm CMOS," in Proc. IEEE Int. Conf. Rebooting Comput. (ICRC), McLean, VA, USA, 2018, pp. 1–7.

[21] G. Csaba, T. Ytterdal, and W. Porod, "Neural network based on parametrically-pumped oscillators," in Proc. IEEE Int. Conf. Electron. Circuits Syst. (ICECS), Monte Carlo, Monaco, 2016, pp. 45–48.